Investigation of directed interaction between neural populations using spectral analysis methods

B.B. Batuev, S.V. Sukhov

***Abstract*—In this work, the mechanisms of directed interaction between two populations of neurons were investigated using spectral analysis methods. The key conclusion of this work is the demonstration that manipulating the background noise level allows the inversion of the direction of information flow between neural populations, opening up new possibilities for controlling functional connectivity in spiking networks. The dynamics of the membrane potentials of two neural populations were modeled based on the "Leaky integrate-and-fire" model. To quantitatively assess the directional information exchange, Granger causality (GC), directional transfer function (DTF), and partial directional coherence (PDC) were used. The results confirm the effectiveness of GC, DTF and PDC for analyzing directed connections in neural networks and justify their use in neurophysiological research. Structural connectivity was generated via an undirected stochastic block model.**

***Key words*— directed transfer function, Granger causality, information flow, partial directional coherence, spiking neural networks**

I. INTRODUCTION

Modern methods of analyzing functional connectivity in neural networks are often focused on assessing directed interactions between groups of neurons, as understanding these connections opens up new pathways for studying the mechanisms of information processing in the brain. One approach to studying such interactions is to use spectral methods for analyzing time series of neural activity, such as Granger causality (GC) [1], directed transfer function (DTF) [2], and partial directed coherence (PDC)[3].

The aim of present work is to conduct a comparative analysis of the effectiveness of GC, DTF, and PDC methods in identifying the direction of information flow between two neural clusters. Within the framework of this objective, the activity of two neural clusters will be simulated at different external stimulus frequencies and noise levels.

The spectral causality indices according to Granger, the directional transfer function, and the partial directional coherence will be calculated on the obtained time series of membrane potential.

GC, DTF, and PDC were selected for our comparative analysis for the following reasons. First, GC provides a clear and quick assessment of the impact based on the logarithm of the ratio of forecast error variances (residuals), which makes the method effective for small sample sizes and a small number of channels [1], [4], [5]. Second, DTF shows not only direct but also cascading flows; specifically, in the case of signal propagation along the path 1→2→3, it also shows signal propagation 1→3 [2], [6]. Third, PDC, by normalizing the columns of the autoregression matrix, identifies only direct connections, which reduces the number of false positive indications of information transfer and facilitates the interpretation of results in complex multidimensional systems [3], [5], [7].

This combination of transparency, sensitivity to the direction of flow, and computational efficiency makes these methods the optimal choice for spectral analysis of directed interactions in simulated spiking neural networks.

II. RELATED WORK

For a more detailed understanding of existing approaches for estimating directed functional and effective connectivity in neural networks, let us review the key methodological developments in this field. In modern neuroscience, a wide range of methodological approaches has been proposed for estimating directed functional connectivity. Among linear parametric methods, classical Granger causality is traditionally applied to time series by simply comparing autoregressive models and estimating the reduction in residual variance when past values of the "causal" series are added [4]. For spectral analysis based on multidimensional autoregressive models, directed transfer function and partial directed coherence are used to identify the direction of information flow in the frequency domain while taking into account the influences of all recording channels [7]. Transfer entropy estimates the directed exchange of information between time series based on entropy measures, which does not require the determination of a specific parametric model

Manuscript received September 05, 2025. This work was supported in part by the Brain Program of the IDEAS Research Center.

Batuev B.B. is with the Kotelnikov Institute of Radio Engineering and Electronics (IRE) of Russian Academy of Sciences, Moscow, 125009, Russia (corresponding author to provide phone: +7-983-451-3009; e-mail: batuyev_bb@cplire.ru).

Sukhov S.V. is with the Ulyanovsk Branch of Kotelnikov Institute of Radio Engineering and Electronics of Russian Academy of Sciences, Ulyanovsk, 432011, Russia (e-mail: ssukhov@ulireran.ru).

and allows the detection of both linear and complex nonlinear dependencies between signals [8]. In addition, there are also phase indicators (phase-locking value, phase-slope index), attractor reconstruction methods (convergent cross mapping), and Bayesian approaches (Dynamic Causal Modeling), each of which has its own advantages and limitations [5].

The role of the noise for the modulation of information flow in neural systems was studies previously in several works. In the work of Cecchi G.A. et al. [9], the authors restore the signal by reducing the noise level. In Gammaitoni L. et al. [10], a classic overview of the phenomenon of stochastic resonance is presented, demonstrating how an optimal noise level can enhance the transmission of weak signals in nonlinear systems. The work by Faisal A. A., Selen L. P. J., Wolpert D. M. [11] describes the functional role of noise in neural networks, including its contribution to improving the reliability of coding and synchronization of neural ensembles. The work by McDonnell M.D., Abbott D. [12] presents a critical analysis of various interpretations of stochastic resonance and discusses its applicability to biological systems, including neural networks. Pikovsky A.S. and Kurths J. [13] describe the phenomenon of "coherence resonance," in which a certain level of noise increases the regularity of spike responses in excitable systems. Ward L. M., MacLean S. E., Kirschner A. [14] conduct an experimental and theoretical study of how noise affects the synchronization of neural populations by changing the direction and strength of information exchange. Each of these works shows that noise is not just a source of fluctuations, but also a mechanism for controlling the direction and efficiency of signal transmission in complex systems.

III. SPIKING NETWORK SIMULATION

As a model system for numerical simulations, we consider spiking neural network. The architecture of the modeled neural network represents an undirected stochastic block model (SBM) [15] consisting of two communities of 50 neurons each (the total number of simulated neurons is $N = 100$). Importantly, the directionality reported by GC/DTF/PDC refers to temporal causal direction, not to the edge orientation of the structural graph. All neurons are described by the leaky integrate-and-fire (LIF) model [16]. The change in the membrane potential of a neuron $v(t)$ is given by the equation:

$$\frac{dv}{dt} = \frac{v_{rest} - v + R \cdot I + v_n + v_e + v_i}{\tau}, \quad (1)$$

where v_{rest} is the steady-state value of the membrane potential, $R = 80\ M\Omega$ is the membrane resistance, I is the external current, $\tau = 20$ ms is the membrane time constant, $v_{n,e,i}$ is the change in the membrane potential caused by synaptic currents from external noise sources and from excitatory e and inhibitory i neurons:

$$v_n += J \sum_n w_n \cdot \delta(t - t_n), \quad (2)$$

$$v_e += J \sum_e w_e \cdot \delta(t - t_e), \quad (3)$$

$$v_i += J \sum_i w_i \cdot \delta(t - t_i). \quad (4)$$

where $J = 1$ mV is a scale factor of a single postsynaptic potential (PSP) that determines the amplitude of the voltage increment; $w_{n,e,i}$ is the strength (weight) of the synaptic contact (dimensionless) for external noise, excitatory, and inhibitory connections, correspondingly; $\delta(t - t_i)$ is the Dirac delta function, modeling an instantaneous voltage jump at the moment of spike; $t_{n,e,i}$ is the moment of spike arrival.

The neuron produces a spike when $v(t)$ reaches the excitation threshold v_{th}, after which the potential is instantly reset to v_{reset}. Formally, this is described by the condition

$$[v(t) > v_{\text{th}}] \Rightarrow v(t + 0) = v_{\text{reset}}. \quad (5)$$

The time dependence of the external current $I(t)$ is specified as a piecewise function:

$$I(t) = \begin{cases} A \cdot \sin(2\pi f_1 t + \phi), & t < 5 \text{ s} \\ A \cdot \sin(2\pi f_2 t + \phi), & t \geq 5 \text{ s} \end{cases} \quad (6)$$

where $f_1 = 10$ Hz and $f_2 = 30$ Hz are the frequencies of sinusoidal currents with amplitude $A = 100$ pA.

Background noise is modeled by two Poisson generators P_1 and P_2. Both generators P_1 and P_2 are connected to communities 1 and 2, respectively, with a probability of $p = 0.3$. The rates $\lambda_1(t)$ and $\lambda_2(t)$ of the occurrence of point events of these Poisson processes are set based on discretized frequency arrays defined at each integration step $\Delta t = \frac{1}{fs}$, where $fs = 100$.

- For t ∈ [0, 5) s: $\lambda_1 = 10, \lambda_2 = 60$
- For t ∈ [5, 10) s: $\lambda_1 = 60, \lambda_2 = 10$

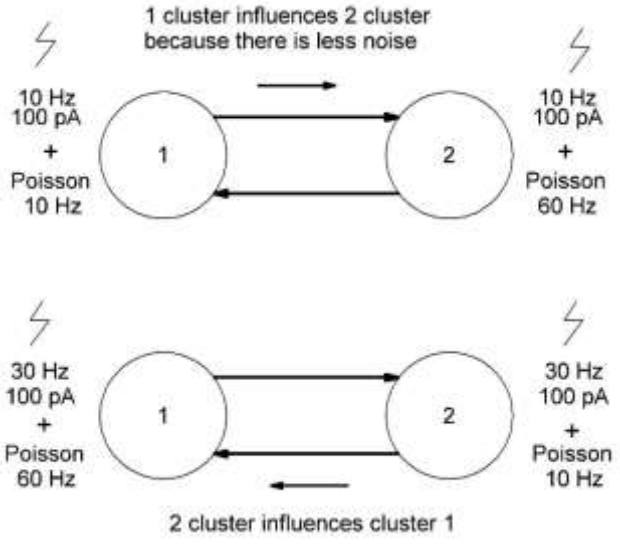

Fig. 1. The scheme of experiment.

Let X denote the number of spikes recorded over a small interval Δt. If the spikes are generated by a Poisson process with a point event rate parameter λ, then X obeys a Poisson distribution:

$$P(X) = \frac{\lambda^x e^{-\lambda}}{x!}, \quad (7)$$

where the mathematical expectation $E[X] = \lambda$ and the variance $\text{Var}(X) = \lambda$. In the context of modeling, this means that, on average, $\lambda \Delta t$ spikes will occur during the time Δt, while their actual number fluctuates around the mean with a standard deviation of $\sqrt{\lambda \Delta t}$.

Let $p_{intra1,2} = 0.15$ be the probabilities of excitatory and inhibitory synaptic connections within the first and second communities, and $p_{inter1,2} = 0.05$ be the probabilities of excitatory and inhibitory synaptic connections between the communities. The weights of the intra- and inter-community connections are equal ($W_{11} = W_{22} = W_{12} = W_{21} = 7$).

Intra- and inter-community connections are divided into excitatory and inhibitory in a ratio of 80:20. Neuron dynamics were modeled using the Brian 2 simulator [17], [18]. The total simulation time was $t = 10$ s.

Having a spiking neural network model for generating time series of membrane potential, we proceed to formalize spectral methods for analyzing directed information exchange.

IV. SPECTRAL ANALYSIS METHODS

After modeling for each time point t, we average the membrane potentials across all the neurons in the first and second communities, forming a two-dimensional time series. To calculate GC, DTF, and PDC, we need to find the spectral power density $S(\omega)$, transfer function $H(\omega)$, and polynomial matrix $A(\omega)$ [18].

Let $y_t = \left(y_t^{(1)}, y_t^{(2)}\right)^T \in \mathbb{R}^k (k = 2)$ is a two-dimensional time series, where $y_t^{(1)}$ is the average membrane potential of community 1, and $y_t^{(2)}$ is the average membrane potential of community 2. Suppose that y_t satisfies a vector autoregression (VAR) model of order $p = 3$ with a constant:

$$y_t = c + \sum_{l=1}^{p} A_l y_{t-l} + u_t,\ u_t \sim \mathcal{N}(0, \Sigma_u). \quad (8)$$

Here, $A_l \in \mathbb{R}^{2\times 2}$ is the matrix of time delay coefficients, $c \in R^2$ is the vector of constant terms, and $\Sigma_u \in \mathbb{R}^{2\times 2}$ is the covariance matrix of Gaussian white noise u_t. We selected the VAR order by minimizing an information criterion in each sliding window and then aggregating the per-window choices. Using a grid $p \in \{1, \dots, 20\}$ and the Bayesian Information Criterion (BIC) [19], which is consistent for order selection, the modal order across windows was $p = 3$.

For two components with frequencies $f_1 = 10$ Hz and $f_2 = 30$ Hz, it is advisable to divide the spectral interval $[f_1, f_2]$ into $N_B \approx 10 - 20$ equal segments with the width Δf. Then

$$N_B = \frac{|f_2 - f_1|}{\Delta f}. \quad (9)$$

Since, for a window span T, the frequency resolution is defined as

$$\Delta f = \frac{f_s}{N} = \frac{1}{T}, \quad (10)$$

we obtain

$$N_B = \frac{|f_2 - f_1|}{\Delta f} = |f_2 - f_1|T = \frac{|f_2 - f_1|T}{f_s} \Longrightarrow T = \frac{N_B f_s}{|f_2 - f_1|}. \quad (11)$$

Substituting $N_B = 10, f_s = 100$ Hz, and $|f_2 - f_1| = 20$ Hz, we obtain $T = \frac{10\cdot 100}{20} = 50$. This rule is valid for a target resolution of $\Delta f = 20$ Hz.

From the sample with window length $T = 50$, we form a matrix of dependent variables

$$Y = \begin{bmatrix} y_p, \\ y_{p+1}, \\ \dots \\ y_{T-1} \end{bmatrix} \in \mathbb{R}^{N\times k}, N = T - p = 50 - 3 = 47. \quad (12)$$

Each lag $l = 1, \dots, p$ forms a block of N rows

$$Y_{-l} = \begin{bmatrix} y_{p-l} \\ y_{p+1-l}, \\ \dots \\ y_{T-1-l} \end{bmatrix} \in \mathbb{R}^{N\times k}. \quad (13)$$

The constant c is estimated as a free column, so the regressor matrix takes the form:

$$X = [1_N\ Y_{-1}\ Y_{-2}\ Y_{-3}\ ] \in \mathbb{R}^{N\times(1+kp)} = \mathbb{R}^{47\times 7}. \quad (14)$$

The least squares method minimizes the expression

$$S(\beta) = \|Y - X\beta\|^2 \quad (15)$$

and leads to the equations:

$$(X^T X)\beta = X^T Y,\ \beta \in \mathbb{R}^{(1+kp)\times k}. \quad (16)$$

The first k elements of β give the estimate $\hat{c}$, the subsequent blocks of k rows are the estimates $A_1, \dots, A_3$.

$$A = \left[B_{1+k(l-1):1+kl}\right]^T,\ l = 1, \dots, p. \quad (17)$$

The residual matrix is formed as:

$$E = Y - X\beta. \quad (18)$$

The unbiased covariance estimate takes into account that $kp + 1$ parameters were estimated, so the number of degrees of freedom is

$$\nu = N - (kp + 1) = 40. \quad (19)$$

The covariance matrix is calculated as

$$\Sigma = \frac{E^T E}{\nu}. \quad (20)$$

We return the coefficient tensor $A \in \mathbb{R}^{3\times 2\times 2}$ and the covariance $\Sigma \in \mathbb{R}^{2\times 2}$.

To transition to the frequency domain, we introduce the ω-transform $y(\omega) = \sum_{t=-\infty}^{\infty} y_t z^{-t}$. Combining all time delays into a polynomial matrix

$$A(\omega) = I - \sum_{l=1}^{p} A_l z^l,\ z = e^{\frac{-j2\pi f}{fs}}, \quad (21)$$

by calculating the invariant, we find the transfer (frequency) matrix, which will be used to find the DTF:

$$H(\omega) = A\left(e^{\frac{-j2\pi f}{fs}}\right)^{-1}. \quad (22)$$

On the unit circle $\omega = e^{-iw}$, the formula gives the spectral power density of the $k \times k$ vector series of the process:

$$S(\omega) = H(\omega)\Sigma H^*(\omega), \quad (23)$$

where the symbol "*" denotes the Hermitian conjugate. The spectral power density can be used to calculate Granger causality.

A. Granger causality

Granger causality (GC) is based on the concept that a time series $y_t^{(1)}$ is considered to be the cause of a time series $y_t^{(2)}$ if including its past values in the regression model for $y_t^{(2)}$ reduces the prediction error compared to a model using only the history of $y_t^{(2)}$.

Consider the two-dimensional case $k = 2$. The total spectral density is written in blocks

$$S(\omega) = \begin{pmatrix} S_{11} & S_{12} \\ S_{21} & S_{22} \end{pmatrix}. \quad (24)$$

To obtain the conditional spectrum used in GC, we first orthogonalize the one-step prediction errors (VAR residuals), thereby removing instantaneous (zero-lag) correlation [1]. For the direction $2 \to 1$, use the upper–triangular transform

$$T_{2\to 1} = \begin{pmatrix} 1 & -s_{12}/s_{22} \\ 0 & 1 \end{pmatrix}, \quad (25)$$

And set $\tilde{\Sigma} = T\Sigma T^T$, $\tilde{H}(\omega) = TH(\omega)$.

The conditional spectrum of $y^{(1)}$ given $y^{(2)}$ is then

$$S_{11|2}(\omega) = \tilde{\sigma}_{11}\left|\tilde{H}_{11}(\omega)\right|^2, \quad (26)$$

Where $\tilde{\sigma}_{11}$ is the (1,1) element of $\tilde{\Sigma}$.

The Granger causality from 2 to 1 is

$$GC_{2\to1}(\omega) = \ln\frac{S_{11}(\omega)}{S_{11|2}(\omega)}. \quad (27)$$

Similarly, for the direction $1 \to 2$ use the lower-triangular transform

$$T_{1\to2} = \begin{pmatrix} 1 & 0 \\ -s_{21}/s_{11} & 1 \end{pmatrix}, \quad (28)$$

so that

$$S_{22|1}(\omega) = \tilde{\sigma}_{22}\left|\tilde{H}_{22}(\omega)\right|^2, \quad (29)$$

and

$$GC_{1\to2}(\omega) = \ln\frac{S_{22}(\omega)}{S_{22|1}(\omega)}. \quad (30)$$

By construction, $GC_{j\to i}(\omega) \geq 0$ indicates that past values of $y^{(j)}$ provide statistically significant predictive information for $y^{(i)}$ at frequency ω.

B. Directed Transfer Function

The directed transfer function (DTF) is also determined based on the same coefficients of the autoregressive model. In the matrix $H(\omega)$, the index i describes how all sources affect y_i. The total energy inflow into the i-th column is equal to $\sum_{m=1}^{k}|H_{im}(\omega)|^2$. Therefore, the value

$$\mathrm{DTF_{ij}}(\omega) = \frac{|H_{ij}(\omega)|}{\sqrt{\sum_{m=1}^{k}|H_{im}(\omega)|^2}}, \quad (31)$$

which quantifies the fraction of the flow from y_j that reaches y_i at frequency ω. Since $H_{ij}(\omega) = A^{-1}(\omega)$, DTF takes into account both direct and all possible indirect paths.

C. Partial directed coherence

Partial directed coherence (PDC) is a further development of the idea of directed analysis, but unlike DTF, it isolates direct (partial) influences between signals, eliminating the contribution of indirect paths through auxiliary variables. To do this, normalization is performed not on the columns of the transfer matrix $H(\omega)$, but on the columns of the polynomial matrix $A(\omega)$. The element $A_{ij}(\omega)$ describes the direct contribution of $y_j(t-(\frac{l}{fs}))$ to $y_i(t)$ with a weight that depends on the frequency. The column vector j has a norm of $\sqrt{\sum_{m=1}^{k}\left|A_{mj}(\omega)\right|^2}$. Then

$$\mathrm{PDC_{ij}}(\omega) = \frac{|A_{ij}(\omega)|}{\sqrt{\sum_{m=1}^{k}|A_{mj}(\omega)|^2}} \quad (32)$$

shows the relative strength of the direct path $j \to i$ at frequency ω compared to all interactions originating from channel j. High PDC values at ω_0 clearly indicate a strong direct influence of source j on receiver i at this particular frequency.

Thus, GC allows us to determine how much taking into account previous values of x_j improves the prediction of the time series x_i as a function of frequency, while DTF analyzes the signal transmission along all possible paths, revealing the frequency characteristics of directed interactions. In contrast, PDC focuses exclusively on direct connections, i.e., cases where the influence of x_j on x_i is expressed directly without taking into account the contribution of other signals. Based on the computational approaches outlined above, the following section presents the results of numerical experiments and the visualization of the signal flow direction.

V. RESULTS

Fig. 2 shows the adjacency matrices with the probability of the connection within clusters 1 and 2 being equal to $P_{intra1,2} = 0.15$ and the probability of a connection between clusters being equal to $P_{inter1,2} = 0.05$.

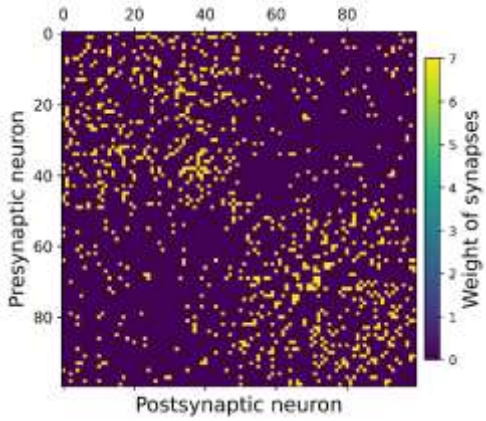

Fig. 2. Adjacency matrix for the simulated neural network.

Fig. 3 shows the example spike activity obtained in the simulation.

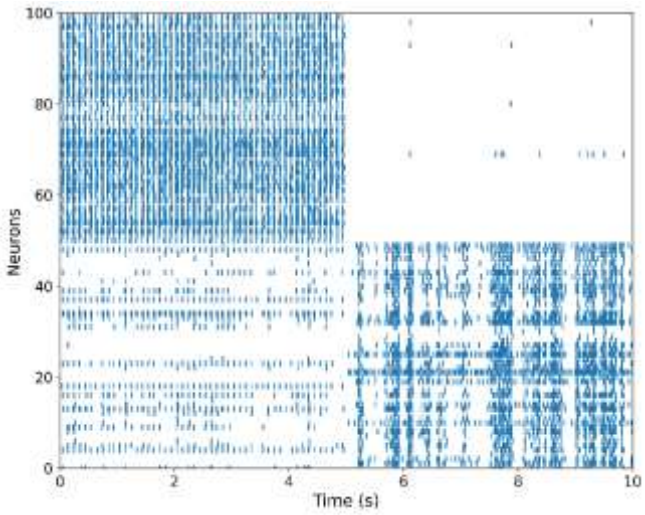

Fig. 3. Spiking activity.

The results of numerical experiments show that neural populations exhibit pronounced oscillations at characteristic frequencies 10 and 30 Hz (see Fig. 4). Until time $t = 5$ s, cluster 1 is more active, generating a clear 10 Hz rhythm, which leads to a strong directed connection $1 \to 2$ at a frequency of $f \approx 10$ Hz. After $t = 5$ s, the situation is reversed: cluster 2 switches to a 30 Hz rhythm, resulting in a bright peak of directed communication $2 \to 1$ at $f \approx 30$ Hz. The noise level determines the direction in which the signals of one cluster affect the signals of another cluster; if the noise is lower, the signal is transmitted better.

The change in the direction of information flows is confirmed by spectral methods (GC, PDC, and DTF) and illustrates how the noise level determines the "direction of information transmission" in the network.

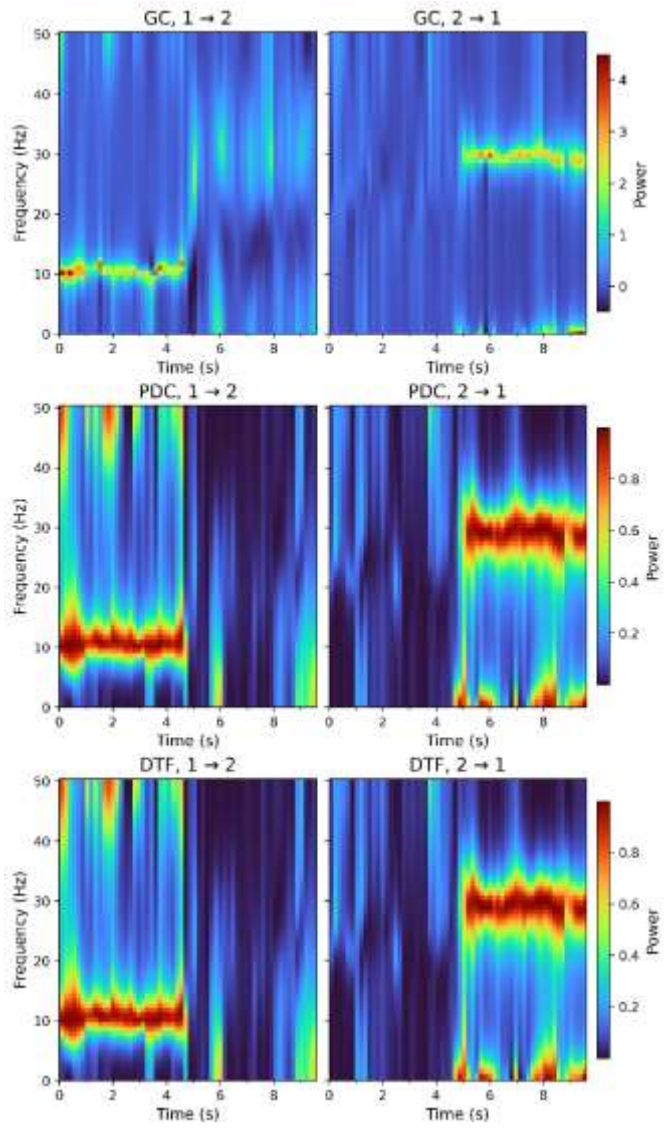

Fig. 4. Spectrograms of a) Granger causality (GC), b) partial directed coherence (PDC), c) directed transfer function (DTF).

VI. CONCLUSION

In conclusion, by regulating the intensity of background noise, it is possible to purposefully change the directionality of information exchange between neural clusters. Numerical modeling and spectral analysis confirmed the high effectiveness of GC, DTF and PDC methods for detecting directional connections in simulated neural populations. The simulation results highlight the role of the network topology parameters and the statistical characteristics of neurons (noise intensity, time constants, synaptic connection weights) in the formation of spectral features of directed interaction. Changes in the noise levels are a key factor capable of reconfiguring the dominant rhythm of a single cluster and reorienting the flow of information.

The conclusions obtained justify the use of DTF and PDC in neurophysiological studies focused on investigating the dynamics of functional and effective connectivity in the brain.

REFERENCES

[1] J. Geweke, "Measurement of linear dependence and feedback between multiple time series," *J Am Stat Assoc*, vol. 77, no. 378, 1982, doi: 10.1080/01621459.1982.10477803.

[2] M. J. Kaminski and K. J. Blinowska, "A new method of the description of the information flow in the brain structures," *Biol Cybern*, vol. 65, no. 3, 1991, doi: 10.1007/BF00198091.

[3] L. A. Baccalá and K. Sameshima, "Partial directed coherence: A new concept in neural structure determination," *Biol Cybern*, vol. 84, no. 6, 2001, doi: 10.1007/PL00007990.

[4] A. M. Bastos and J. M. Schoffelen, "A tutorial review of functional connectivity analysis methods and their interpretational pitfalls," 2016. doi: 10.3389/fnsys.2015.00175.

[5] B. Batuev and S. Sukhov, "Determining the directions of information flow between populations of spiking neurons," in *2024 X International Conference on Information Technology and Nanotechnology (ITNT)*, 2024, pp. 1–5. doi: 10.1109/ITNT60778.2024.10582395.

[6] M. Kaminski and K. J. Blinowska, "Directed Transfer Function is not influenced by volume conduction-inexpedient pre-processing should be avoided," 2014. doi: 10.3389/fncom.2014.00061.

[7] K. J. Blinowska, "Review of the methods of determination of directed connectivity from multichannel data," 2011. doi: 10.1007/s11517-011-0739-x.

[8] R. Vicente, M. Wibral, M. Lindner, and G. Pipa, "Transfer entropy-a model-free measure of effective connectivity for the neurosciences," *J Comput Neurosci*, vol. 30, no. 1, 2011, doi: 10.1007/s10827-010-0262-3.

[9] G. A. Cecchi, M. Sigman, J. M. Alonso, L. Martínez, D. R. Chialvo, and M. O. Magnasco, "Noise in neurons is message dependent," *Proc Natl Acad Sci U S A*, vol. 97, no. 10, 2000, doi: 10.1073/pnas.100113597.

[10] L. Gammaitoni, P. Hänggi, P. Jung, and F. Marchesoni, "Stochastic resonance," *Rev Mod Phys*, vol. 70, no. 1, 1998, doi: 10.1103/revmodphys.70.223.

[11] A. A. Faisal, L. P. J. Selen, and D. M. Wolpert, "Noise in the nervous system," 2008. doi: 10.1038/nrn2258.

[12] M. D. McDonnell and D. Abbott, "What is stochastic resonance? Definitions, misconceptions, debates, and its relevance to biology," 2009. doi: 10.1371/journal.pcbi.1000348.

[13] A. S. Pikovsky and J. Kurths, "Coherence Resonance in a Noise-Driven Excitable System," *Phys Rev Lett*, vol. 78, no. 5, 1997, doi: 10.1103/PhysRevLett.78.775.

[14] L. M. Ward, S. E. MacLean, and A. Kirschner, "Stochastic resonance modulates neural synchronization within and between cortical sources," *PLoS One*, vol. 5, no. 12, 2010, doi: 10.1371/journal.pone.0014371.

[15] P. W. Holland, K. B. Laskey, and S. Leinhardt, "Stochastic blockmodels: First steps," *Soc Networks*, vol. 5, no. 2, 1983, doi: 10.1016/0378-8733(83)90021-7.

[16] N. Brunel and M. C. W. Van Rossum, "Lapicque's 1907 paper: From frogs to integrate-and-fire," *Biol Cybern*, vol. 97, no. 5–6, 2007, doi: 10.1007/s00422-007-0190-0.

[17] M. Stimberg, R. Brette, and D. F. M. Goodman, "Brian 2, an intuitive and efficient neural simulator," *Elife*, vol. 8, 2019, doi: 10.7554/eLife.47314.

[18] H. Lütkepohl, *New introduction to multiple time series analysis*. 2005. doi: 10.1007/978-3-540-27752-1.

[19] G. Schwarz, "Estimating the Dimension of a Model," *The Annals of Statistics*, vol. 6, no. 2, 2007, doi: 10.1214/aos/1176344136.